Fabrig: A Cloth-Simulated Transferable 3D Face Parameterization

CHANGAN ZHU, School of Information Technology, Carleton University, Canada
CHRIS JOSLIN, School of Information Technology, Carleton University, Canada

Fig. 1. Four examples of Fabrig parameterized 3D faces and their animated result.

Existing 3D face parameterization methods are limited to human faces and/or require a large amount of manual work to prepare face-specific blendshapes. Unfortunately, many of the automated parameterization methods do not provide local controls for the different facial regions and methods that allow the integration of physics-based simulations also suffer from limited character compatibility and editability. We propose a human face anatomy-inspired 3D face parameterization method called Fabrig, which is quick to set up, transferable among various characters, easily editable, and compatible with physics-based simulations. Instead of using conventional volume-centric simulation for the face anatomy, our method innovatively uses cloth simulation for lighter computation. The parameterized faces support physics-based effects like collision and show skin details such as dynamic wrinkles. From our objective evaluation, we found that our method can parameterize the faces of various characters, ranging from realistic humans to non-humans, without any labor-demanding preparation work. The parameterized faces can be edited at the anatomical level while remaining intuitive to artists. Our evaluation results confirm that this new parameterization can accurately and naturally recreate the facial poses of a character or facial actions performed by a motion capture subject.

CCS Concepts: • **Computing methodologies → Animation**.

Additional Key Words and Phrases: 3D Face Parameterization, 3D Face Rigging, Character Animation, Visual Effects, Motion Capture, Retargeting

Authors' Contact Information: ChangAn Zhu, School of Information Technology, Carleton University, Canada, leazhu@cmail.carleton.ca; Chris Joslin, School of Information Technology, Carleton University, Canada, chrisjoslin@cunet.carleton.ca.

SA Conference Papers '24, December 03–06, 2024, Tokyo, Japan

ACM ISBN 979-8-4007-1131-2/24/12
https://doi.org/10.1145/3680528.3687695

ACM Reference Format:
ChangAn Zhu and Chris Joslin. 2024. Fabrig: A Cloth-Simulated Transferable 3D Face Parameterization. In *SIGGRAPH Asia 2024 Conference Papers (SA Conference Papers '24), December 03–06, 2024, Tokyo, Japan.* ACM, New York, NY, USA, 10 pages. https://doi.org/10.1145/3680528.3687695

1 Introduction

3D characters have been widely used in the production of films, games, advertisements, and interactive systems, yet the pipeline to create 3D characters is still labor-demanding [Cao et al. 2013; Choe et al. 2001; Choi et al. 2022] and the parameterization or rigging of a 3D face has been a long-existing challenge. Humans are sensitive to facial motions, if a realistic human character performs anatomically inappropriate facial motion, viewers can feel uncomfortable, namely, the facial movements fall into the Uncanny Valley [Mori 1970]. Facial details such as wrinkles, creases, and folds contribute largely to the characteristics of a face and the conveyance of a character's subtle emotions. Therefore, in production, face parameterization methods that constrain facial movements within an appropriate range and present facial details are preferable. Specifically, the blendshape parameterization model [Lewis et al. 2014] is one of the most widely used production methods. However, since blendshape models build upon facial actions prepared for the same face geometry, they can have overlapping influences on some facial regions when multiple blendshapes are activated; they are also labor-intensive to prepare. Methods such as 3D Morphable Models (3DMM) [Blanz and Vetter 2023] do not pose such limitations. However, since the 3DMM is usually constructed using datasets of human face scans, its generated face instances are limited to realistic human characters [Cao et al. 2013; Egger et al. 2020; Qin et al. 2023; Wu et al. 2023]. Other work that uses the anatomical components (e.g., muscles, fat, skin) of a face combined with physics-based simulation or geometric deformation to simulate their behaviors [Choi et al. 2022; Ichim et al. 2016; Waters 1987] are known as anatomy-inspired models. Yet, models based on deformation [Orvalho et al. 2008] present facial animation with limited quality. Physics-based models provide high-fidelity facial animation [Choi et al. 2022; Cong et al. 2015; Ichim et al. 2017; Yang et al. 2023] but are mostly volume-based. Therefore, they are computationally heavy and hard to control. In addition, many of these physics-based models largely rely on face scans or face-specific blendshapes to guide the simulation [Barrielle et al. 2016; Ichim et al. 2016].

Proposed Method. Our method (Figure 1) expands on the anatomy-inspired physics-based face models but effectively removes the restrictions imposed by volumetric components. Our proposed face parameterization utilizes abstracted facial muscles and their local deformation spaces to create facial poses. The physics-based properties of a face are innovatively realized using the cloth simulation [Baraff and Witkin 2023]. Specifically, we generate surface-based meshes as skull, muscle, and fat patches from a normalized 3D face, transfer a set of template muscle blendshapes to the muscle patches, and then use the muscle blendshape weights to control each muscle's deformation. The rigid motion of the muscles and fat patches is handled by the skull mesh and the secondary motion is automatically generated using cloth simulation. Since any normalized 3D face can be used to generate the same set of patches, this parameterization is transferable to a wide range of character faces.

Contributions. Our main contributions are:

- An anatomy-inspired face parameterization method that models the facial muscles and fat pads relating to expressions.
- A parameterization method that is independent of face-specific blendshapes and capable of presenting natural and semantically accurate facial actions across human, human-like, and even non-human characters.
- An innovative solution that uses cloth simulation to mimic the physics-based properties of the facial muscles and fat, allowing effects like collision and inertia, reaction to fields like wind and gravity, and automatically creating skin details like dynamic wrinkles.
- Parameterized faces can be easily edited by manipulating the muscle blendshapes and driven by facial motion capture data or an animated face when rigged using the Facial Action Coding System (FACS) [Ekman and Friesen 1978].

2 Related Works

Existing methods for 3D face parameterization can be divided into three main categories – blendshape models, 3D morphable models, and anatomy-based models. We also discuss the new arising concept - neural face models, which take inspiration from these three categories, within the corresponding sections.

Blendshape. Blendshape parameterization is based on geometric morphology, where a 3D face with a neutral expression is duplicated and modified to represent the various facial actions in a set of face variants (i.e., blendshapes), and a weighted linear combination of these face variants generates believable facial animation.

Research that inspired our method, within this category, is from Wu et al. [Wu et al. 2016] and Chandran et al. [Chandran et al. 2022]. Wu et al. [Wu et al. 2016] proposed a local blendshape model that models 3D faces with patches extracted from the face mesh and defined these patches' local deformation using the expression meshes (similar to blendshapes) reconstructed from monocular videos. This method has been extended by Gruber et al. [Gruber et al. 2020] for interactive editing of a 3D face and by Chandran et al. [Chandran et al. 2022] using 20 blendshapes to define the deformation spaces of the patches for high-quality retargeting. For blendshape models in general, creating face-specific blendshapes or cleaning up the equivalent 3D scans is labor-intensive [Zhang et al. 2020]. In addition, though blendshape parameterization can control the deformation of a face within a relatively appropriate range by constraining the weighted sum of blendshapes [Lewis et al. 2014], it does not guarantee the visual plausibility or the expressiveness of facial actions [Seol et al. 2012]. Blendshapes are proven to be statistically correlated [Lewis et al. 2014], which can result in over-deformation [Ribera et al. 2017] or cancelling effects in certain facial regions [Orvalho et al. 2012].

3D Morphable Models (3DMM). The 3DMM learns a statistical model of 3D faces from datasets of face scans [Blanz and Vetter 2023]. 3DMM extracts variations from the face datasets using linear methods like the Principal Component Analysis (PCA) or nonlinear methods like deep-learning models; these variations are statistically independent. Therefore, a 3DMM is less likely to generate facial actions beyond the limit of human facial anatomy [Zhu and Joslin 2024].

Since the variations extracted by PCA are not perceptually understandable [Egger et al. 2020], recent research uses a combination of PCA and nonlinear methods to decouple the perceptually understandable variations in a face dataset (e.g., the variations from expressions, identities, and poses) [Li et al. 2017] or to explore the connection between the variations and other cues like neck bones [Zhang et al. 2023] or skull shape [Qiu et al. 2022]. More examples of this integration of nonlinear methods in 3DMM include parameterizing 3D faces using face images under different poses and illumination conditions [Tran and Liu 2018], deep-learning models like Variational Auto Encoders [Bagautdinov et al. 2018; Paier et al. 2023; Zhang et al. 2022], and Generative Adversarial Networks [Abrevaya et al. 2019]. 3DMM has also been used to reenact faces in images and videos [Thies et al. 2015], perform motion retargeting between realistic 3D faces [Chaudhuri et al. 2020; Zhang et al. 2022], and generate faces with high-frequency details [Bao et al. 2021; Li et al. 2020]. However, 3DMM is limited in that it relies on well-constrained training datasets for robust 3D face modelling, and the applicable range of characters is limited to the faces of real human or their instances due to its learning nature.

Anatomy-based. Anatomy-based parameterization focuses on modelling the behaviors of the facial anatomical components (e.g., skull, muscles, fat, etc.), and the animation is generated through physics-based simulation, geometric deformation of these anatomical components, or the learned relation between the face deformation and the anatomical components.

The idea of using physics to simulate human facial anatomy was first proposed by Waters [Waters 1987], who suggested simulating muscle behaviors using a mass-spring system. The model was later extended to consider other relevant anatomical components of a face such as the cutaneous and subcutaneous tissues [Terzopoulos and Waters 1990]. Physics-based simulation can provide realistic facial animation and allows a face to respond to external forces or interact with objects, but is not as easy to control a specific facial region [Ichim et al. 2016]. Therefore, deformation-based methods have been developed by researchers in both academia and industry [Blender 2023; Marcos et al. 2008; Umenhoffer and Tóth 2012] that utilize joints to imitate facial muscle movements; however, as the joints have fixed weight influence on the face mesh, the presented facial poses are not always natural.

The possibility of fusing the advantages of physics-based simulation and deformation has also been explored. Researchers have investigated using blendshapes or face scans to guide the simulation of a tetrahedralized face volume [Ichim et al. 2016; Sifakis et al. 2005] and using the morphing from one blendshape to another to simulate the muscle forces and deforming a face mesh [Barrielle et al. 2016]. Others have attempted using blendshapes or face scans to establish correspondences between explicit [Bao et al. 2019; Choi et al. 2022; Ichim et al. 2017] or implicit muscle activation and tetrahedralized face volumes [Srinivasan et al. 2021; Wagner et al. 2023; Yang et al. 2022] or face surface deformation [Chandran and Zoss 2024]. Some research even modelled the subtle variation from expression style [Yang et al. 2023]. These methods usually provide high-fidelity facial animation, while their common limitation is that they need existing face scans or blendshapes to guide the simulations, which are again time-consuming to prepare. A method proposed by Cong et al. [Cong et al. 2015], defined a blendshape model for the muscles and simulated their influence on the tetrahedralized flesh volume, enabling a highly directable parameterization and has been applied in production [Cong and Fedkiw 2019]. This method is more flexible for the different types of characters and is independent of face-specific blendshapes.

Two methods closest to ours are from Chandran et al. [Chandran et al. 2022] and Cong et al. [Cong et al. 2015]. However, unlike Chandran et al. [Chandran et al. 2022], whose local blendshape model is not compatible with physics-based simulation and Cong et al. [Cong et al. 2015] that utilized volume-based simulation for faces, we enable physics-related behaviors of 3D faces on the surface-based anatomical components. Specifically, since facial muscles are typically thin and unstable when simulated by tetrahedrons [Cong 2016; Ichim et al. 2017], we mimic their physics-based properties with cloth simulation, which is lightweight and more stable. The face volume is preserved by the rigid-body simulation of the skull and the deformation spaces of the muscle patches.

3 Design Objectives

Based on the standards set out in the state-of-the-art, we have designed a new 3D face parameterization method - Fabrig, with objectives focusing on production efficiency, artistic control, flexibility, and fidelity [Moser et al. 2021; Seol et al. 2011]:

Fast parameterization. The time needed to parameterize a 3D face using conventional blendshape-based methods ranges from weeks to months [Baker 2019]. Our goal for Fabrig is to reduce the time to less than a day.

Transferable across different character types. Most existing 3D face parameterization methods that do not require blendshapes or face scans, have limited transferability to non-human characters (e.g., monsters, goblins). Our aim for Fabrig is for it to be capable of parameterizing such faces.

Physics-based properties. The capability of face parameterizations to show physics-based effects is an important factor for high-fidelity facial animation [Ichim et al. 2017; Yang et al. 2023]. Therefore, the Fabrig parameterized face should be able to show physics-based properties such as collision and field reaction (e.g., gravity).

Editable and drivable by facial performance. In production, the parameterized faces need to be editable with tools that rigging artists are familiar with. With the increasing demand for character animation fidelity, the visual effects and film industry have been extensively using live-action performance to drive facial animation. Therefore, Fabrig-parameterized faces should be easily drivable by facial motion data.

Visually plausible. Research has shown that if viewers feel uncomfortable about a face or its animation, the information that can be effectively delivered by that character is significantly reduced [Mori 1970; Shin et al. 2019]. Hence, faces parameterized by Fabrig need to present natural facial actions.

Present accurate semantic information. When comparing the facial actions performed by a mocap subject and the actions being applied to their parameterized 3D face, the faces should be able to present actions that share the same semantic information (i.e., meaning and intensity) as the actions performed by the mocap subject.

4 An Anatomy-inspired Face Parameterization

4.1 Face Anatomy

To parameterize 3D faces based on facial anatomical components, it is important to understand facial anatomy. Human faces are composed of the skull, muscles, fat pads, ligaments, and skin. The facial muscle is a key component of face anatomy, whose active contraction leads to the global movements of the jaw and the passive movements of the other muscles, fat pads, and skin. The facial muscles relating to expressions are mostly anchored at the skull and are attached to the skin or other muscles. The fat pads and skin are attached to the muscles or the skull membrane by ligaments. For facial regions with fat pads, the contraction of muscles results in bulging or wrinkling. Although research has revealed that the jaw movement is non-linear [Zoss et al. 2018], a linear rotation can reflect most of its common movements [EpicGames 2023]. The facial muscle behaviors are more complex, they can be categorized into the "linear" muscles that pull along one direction, and the "sphincter" muscles that squeeze, roll, open, and close [Waters 1987].

4.2 Fabrig Components and Pipeline

Fabrig uses a set of abstracted anatomical components – the skull, muscles, and fat pads that have large influences on expressions; all represented as simple mesh patches. We consider the original 3D face mesh as the skin, which aligns with the character rigging conventions in production.

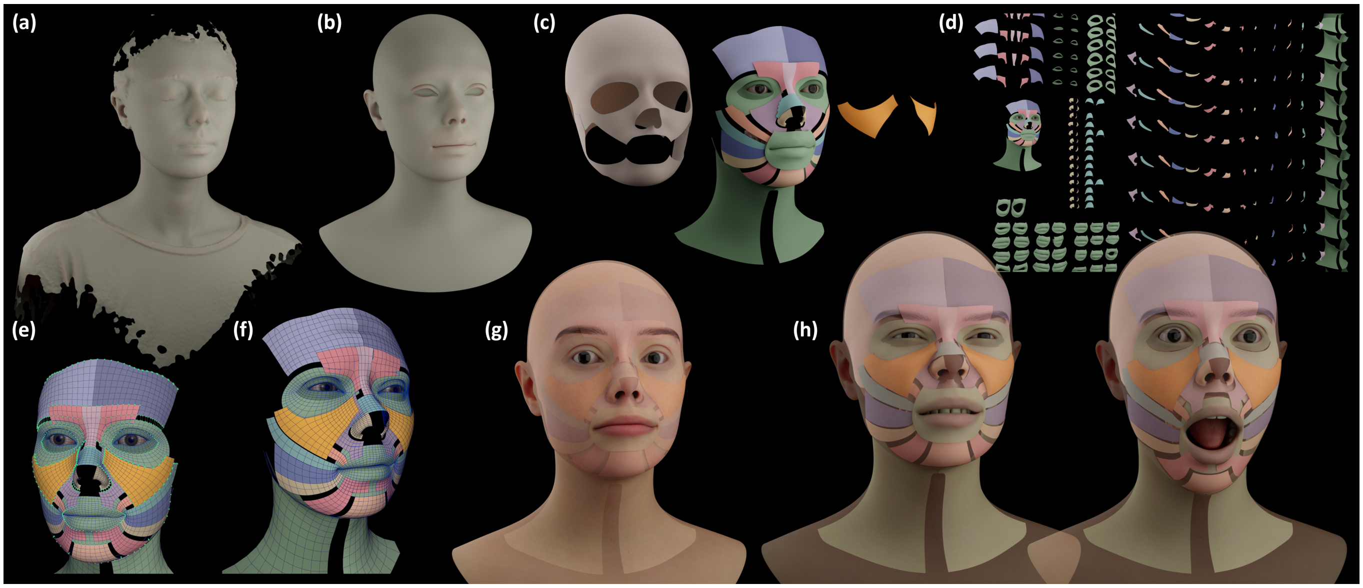

Fig. 2. Fabrig components and pipeline. (a) Face mesh to be normalized, (b) normalized face mesh; (c) anatomical components; (d) template muscle blendshapes; (e) attachment constraints (green dots) as ligaments; (f) apply cloth simulation to the muscle and fat patches and attracting the muscle cloth to the muscle blendshapes; (g) create weighted influences from the patches to the skin; (h) pose or animate this face by manipulating the muscle blendshape weights.

To parameterize a 3D face with Fabrig, we start by registering the face mesh to a template mesh, which normalizes the face mesh so that it shares the same topology with the template (Figure 2.a to b). This can be achieved using the same registration process as in the FaceWarehouse [Cao et al. 2013], FLAME [Li et al. 2017], or FaceScape [Yang et al. 2020]. Then, we generate the anatomical components from the normalized face mesh based on a predefined patch template (Figure 2.c), representing the skull, facial muscles, and fat pads.

After that, we transfer a set of template blendshapes to the generated muscle patches to create their local deformation spaces (Figure 2.d), as detailed in Section 4.3. Following that, we attach these muscle patches to the skull and fat patches to the muscles (Figure 2.e) and simulate the muscle patches as cloth and constrain them to their original deformation spaces through a magnetic constraint (Figure 2.f), as detailed in Section 4.4. Finally, we overlay the skin mesh on top of the anatomical components, where these anatomical components have weighted influences on the skin mesh vertices based on Euclidean distances (Figure 2.g) and deform the skin as they move (Figure 2.h). The skin mesh deforms with its underlying muscle and fat patches and shows all physics-based behaviors presented by these patches accordingly, therefore they will not be penetrated during interactions like colliding objects.

4.3 Muscle Patches and Transferable Blendshapes

Since the a normalized face mesh shares the same topology with the template mesh, the patches generated from it are also consistent in topology with the template patches, which enable the transfer of the template muscle blendshapes to the muscle patches of different faces. The template muscle blendshapes reflect the facial muscles' active contractions and passive actions caused by other muscles (Figure 2.d). For the muscle group around the eyes, we do not explicitly model the inner eye muscles such as Levator Palpebrae Superioris, Superior rectus, and Superior Tarsal, but embed their influences on the eye movement into the passive actions of the eye surface muscle Orbicularis Oculi, which allows a modelling focusing on the face surface. Similarly, we embed the face surface movements from Corrugator Suppercilii into Depressor Supercilii and movements from Levator and Depressor Anguli Oris into Orbicularis Oris. Since Fabrig extracted muscle patches share topology across different faces, we only need to create these template muscle blendshapes once and they can then be transferred to muscle patches extracted from any normalized 3D face.

Equation 1 denotes the shape of a template muscle patch X_p^t that has N template blendshapes, which is mathematically analogous to a blendshape model:

$$X_p^t = b_0^t + \sum_{i=0}^{N-1} w_i \Delta b_i^t, \tag{1}$$

where Δb_i^t represents the offset between the template muscle blendshape and its neutral status, and w_i is the blendshape weight. Δb_i^t is expressed in Equation 2:

$$\Delta b_i^t = b_i^t - b_0^t, \tag{2}$$

where b_0^t is the neutral shape of the template muscle patch X_p^t, and b_i^t is a blendshape of X_p^t.

With shared topology across the muscle patches in different faces, the blendshapes of the template muscle patch can be easily transferred to the muscle patches of another face through linear morphing transfer [Blanz et al. 2003]. This process can be considered as adding

Δb_i^t to the neutral shape of the corresponding muscle patch of a new face. However, muscles of different face sizes might have a different deformation scale. For example, the various jaw-opening angles of different characters can result in a varied scale of muscle patch deformation around the mouth. Therefore, we introduce a scalar parameter α to modify the amount of morphing being transferred to the muscle patch of a new face, where a muscle patch shape can be described using Equation 3:

$$X_p = b_0 + \alpha \cdot \sum_{i=0}^{N-1} w_i \Delta b_i^t, \tag{3}$$

where b_0 is the neutral shape of the new face's muscle patch, α is the patch-specific morphing transfer scalar that can be empirically provided by rigging artists or automatically optimized. For 3D face meshes without whole-face blendshapes or expression scans, we set $\alpha > 1$ when the new muscle patch is bigger than the template muscle patch and $\alpha < 1$ when it is smaller than the template. For face meshes with blendshapes or expression scans, we use the α values that generate poses with the smallest Mean Squared Error (MSE) from those blendshapes or scans. The blendshape weight is denoted as w_i, and Δb_i^t as the blendshape offset from the template muscle patch. This property embeds the influence of the global rotation of the jaw into the deformation of the muscle patch, which further guarantees the robustness of Fabrig in terms of preserving the meaning and intensity of a facial action when using it for a scenario like motion retargeting.

4.4 Cloth-Simulated physics-based properties

After defining Fabrig and the local deformation spaces of its muscle patches, it is also important to enable the passive movements of the fat patches and the secondary motion of the muscles. These require the physics-based simulation of the anatomical components.

In methods aiming for accurate physics-based simulations, like Finite Element Methods (FEM) [Zienkiewicz and Taylor 2000], the positions of particles on a dynamic object are updated based on the forces applied to them, and the simulation is realized by explicitly minimizing the total energy of this object at each time point. This type of simulation, when applied to simulating facial anatomical components, is usually volume-based [Sifakis et al. 2005], which is closer to actual physics but can suffer from a long simulation time [Ichim et al. 2017].

Our method utilizes Position-Based Dynamics (PBD) [Müller et al. 2007] to simulate the physics-based properties of the muscle and fat patches through a surface-based nCloth solution [Stam 2009]. For each cloth, instead of computing the new position of its vertices at each time point based on forces, nCloth modifies its vertices' positions to satisfy a set of constraints, therefore simulating the cloth behaviors. Specifically, it first predicts the new positions for the vertices based on external forces like gravity and wind, then updates the predicted new positions to let the vertices satisfy a set of constraints, resulting in their final positions at the current time point. These constraints are mathematical conditions creating physics-based effects (e.g., stretch, shear, bend, and collision) on the cloth when they are satisfied, and the process of satisfying these

Algorithm 1 Position Based Dynamics Algorithm

1: **for** all vertices i **do**
2: initialize $M_{p,i} \leftarrow M_{p,i}^0$, $v_i \leftarrow v_i^0$
3: **end for**
4: **loop**
5: **for** all vertices i **do**
6: $v_i \leftarrow v_i + \Delta t f_{\text{ext}}(M_{p,i})$
7: **end for**
8: dampVelocities($v_1, \ldots, v_N$)
9: **for** all vertices i **do**
10: $p_i \leftarrow M_{p,i} + \Delta t v_i$
11: **end for**
12: **for** all vertices i **do**
13: generateCollisionConstraints($M_{p,i} \rightarrow p_i$)
14: **end for**
15: **for** solverIterations times **do**
16: projectConstraints($C_1, \ldots, C_{M+M_{\text{coll}}}, p_1, \ldots, p_N$)
17: **end for**
18: **for** all vertices i **do**
19: $v_i \leftarrow \frac{p_i - M_{p,i}}{\Delta t}$
20: $M_{p,i} \leftarrow p_i$
21: **end for**
22: velocityUpdate($v_1, \ldots, v_N$)
23: **end loop**

constraints implicitly minimizes the total energy of the cloth. Therefore, PBD-based cloth simulation can work in real-time. Applying this idea in the Fabrig simulation, we use a cloth version of the muscle patch X_p, termed "muscle cloth" M_p. Assuming M_p consists of N vertices and has M constraints, each vertex $M_{p,i}$ has unit mass and a velocity v_i, we can simulate M_p based on the PBD process as shown in Algorithm 1 [Müller et al. 2007]. The detailed definitions of velocity damping (Algorithm 1, Line 8), collision constraints' generation (Line 13), and constraints projection (Line 16) can be found in the work of Müller et al [Müller et al. 2007].

The key step for presenting the physics-based properties is shown in Algorithm 1, Line 16, which updates the positions of all vertices to satisfy the constraints. Aside from the constraints for cloth behaviors like stretch, shear, bend, and collision, our focus is to allow the local deformation space of each muscle patch to influence its corresponding muscle cloth. Therefore, we create a magnetic constraint C_{mag} for each vertex on the muscle cloth M_p to attract it to the corresponding vertex on X_p at each frame. This magnetic constraint is specified in Equation 4:

$$C_{mag}(i) = ||X_{p,i} - M_{p,i}||, \tag{4}$$

which is essentially a constraint to minimize the vertex distances between the muscle cloth M_p and its actual shape X_p. For each M_p, it is attracted by the deformation of the muscle patch X_p, and other constraints also react to this attraction. Note that this magnetic constraint is different from warping [Milliron et al. 2002] as it takes part in the simulation and influences the physics-based behaviors of the muscle cloth, i.e., if the muscle patch contracts at high speed, the muscle cloth exhibits a "jiggling-wiggling" effect as a dynamic object, which warping is not capable of. Since fat patches move passively, we stitch them to muscle patches through attachment constraints (Figure 2.e) and their deformation follows the movements of the muscle patches. These attachment constraints are similar to the magnetic constraints:

$$C_{attch}(i, j) = ||A_i - M_{p,j}||, \tag{5}$$

where A_i is a vertex on the mesh that is being attached, for instance, a vertex on the skull and $M_{p,j}$ is a vertex on the muscle cloth M_p.

The integration of cloth simulation enables physically interactive animations for the Fabrig parameterized faces (Figure 2.f). If we set the face to have loose skin by manipulating the parameters of the cloth, the patches automatically generate wrinkles (Figure 3.a). When sphincter muscles like Orbicularis Oris (the circular-shape muscle around the mouth) contract, the collision constraint shows their stickiness (Figure 3.b) and prevents geometric intersection (Figure 3.c). In addition, we use rigid-body simulation for the skull to ensure the head volume does not drastically change. The muscle volumes are preserved by the muscle blendshapes and the magnetic constraints, which hold the muscle patches so their primary deformation is within the range of the muscle's local deformation space. For the fat patches, we apply a small amount of air pressure, so their volumes remain even with the gravity direction changes (e.g., when the character lies down).

Table 1. The simulation setup and runtime of 19.4k vertices

Action Complexity	Detect Collision	Runtime (FPS)
Simple	Sphincter muscles only	37.329
Simple	All patches	32.866
Complex	Sphincter muscles only	35.268
Complex	All patches	29.710

Since the simulation is surface-based, it is computationally efficient, the simulation for the anatomical components of 19.4k vertices runs in real-time on a consumer-level PC with an AMD Ryzen 9 7900 processor, 32 GB of RAM, and a GeForce RTX 4070 Ti graphics card. We include the detailed simulation time in Table 1, where the simple actions are manually animated poses with a few muscles activated and the complex actions are from mocap data with all muscles activated. The implementation of the muscle and fat simulation can be achieved using the nCloth simulation, we provide details of the relevant parameters in Table 2 as a reference.

5 Evaluation

We evaluated Fabrig from both objective and subjective perspectives.

5.1 Data Preparation

As part of the evaluation, we prepared a set of facial actions and two sets of 3D faces as follows:

Table 2. The nCloth parameters setting reference

Parameters	Linear Muscles	Sphincter Muscles	Fat Pads
Mass	1.00	1.00	1.00
Stretch resistance	10.00	10.00	8.00
Bend resistance	5.00	5.00	3.00
Compression resistance	10.00	10.00	8.00
Bend angle dropoff	0.30	0.20	0.30
Overall damping	0.72	0.72	1.50
Stretch damping	0.10	0.10	0.20
Pressure	-	-	0.30

Facial Action Set. This set contains the video recordings and mocap data of five live-action subjects, covering the seven universally recognizable facial expressions of emotions [Matsumoto and Ekman 2008] (happy, sad, surprise, fear, anger, disgust, and contempt) and their random performances. The five subjects have a large variation in bone structure and facial proportion.

3D Scan Face Set. This set contains the static face scans of the same five live-action subjects' neutral expression.

Character Face Set. This set contains five faces of 3D characters, covering one realistic human character, two realistic human-like characters, and three realistic non-human characters.

5.2 Objective Evaluation

For the objective evaluation, our goal was to evaluate Fabrig's expression recreation capabilities across the various character categories. Therefore, we utilized the *Character Face Set* and compared the accuracy of the recreated pose between our Fabrig method and whole-face delta transfer method (which was used by Chandran et al. [Chandran et al. 2022] for their evaluation).

Using four blendshapes from each face as the ground truth data, we computed the mesh differences between the blendshapes and the equivalent poses recreated by Fabrig and whole-face delta transfer, all faces were scaled to the true size of a human head. Table 3 presents the mean mesh differences and their standard deviations. As can be observed from Table 3, Fabrig presents a smaller mesh difference from the faces' blendshapes than whole-face delta transfer method in three out of four cases.

Table 3. The mesh difference across the four blendshapes using delta transfer vs. Fabrig

Blendshapes	Delta-transfer (mm)	Fabrig (mm)
Mouth corners up	1.085±0.099	**0.896±0.075**
Eyebrows down	1.033±0.119	**0.943±0.106**
Mouth open	1.253±0.153	**0.981±0.103**
Sneer	**1.010±0.103**	1.029±0.127

According to our design objectives as specified in Section 3, we also report the parameterization time, transferability, physics-based properties, editability, and performance drivability of Fabrig.

Parameterization Time. Across the ten faces in the two face sets, the process of Fabrig parameterization takes on average 33 min 6 sec with a standard deviation of 2 min 56 sec including the 3D face normalization process. Although it is longer than the commercial face rigging application MetaHuman Creator [EpicGames 2023], which averaged 25 min 48 sec with a standard deviation of 6 min 48 sec, Fabrig is still more than 30 times faster compared to the blendshape-based rigging process in production, which usually takes weeks or months [Baker 2019].

Transferability. Fabrig demonstrates high flexibility when being transferred to different faces. It can parameterize 3D faces ranging from realistic human characters to non-human characters. Figure 6 contains three Fabrig parameterized character faces being applied with the same muscle blendshape weights. The three faces show semantically equivalent expressions without manual adjustment and the expression on each face fits their size and proportion.

Physics-based Properties. Since we integrated cloth simulation in Fabrig, the parameterized faces present physics-based effects like collision (Figure 3) and inertia, and react to fields like gravity and wind.

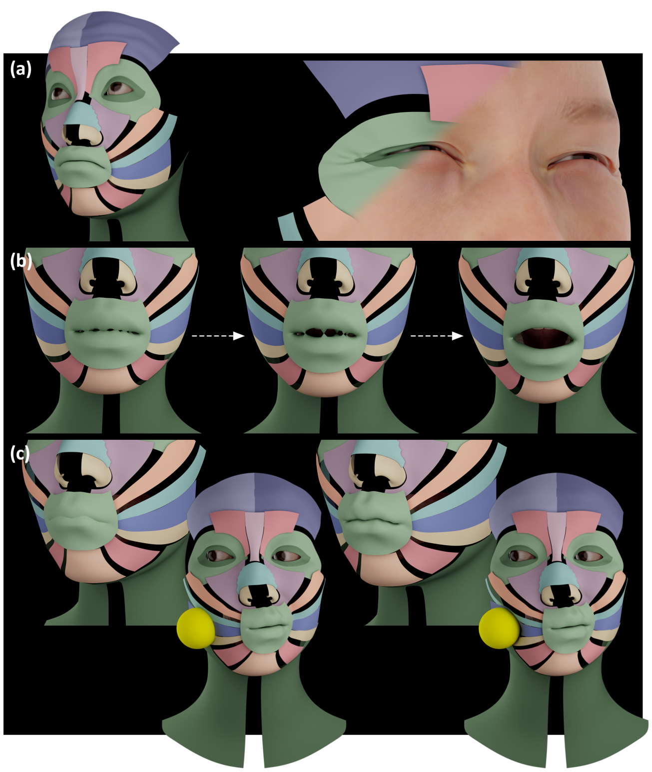

Fig. 3. The physics-based properties realized by Fabrig. (a) Dynamic wrinkles in the forehead and around the eyes, (b) lips stickiness when the mouth opens, and (c) a comparison between collision off (left) and collision on (right).

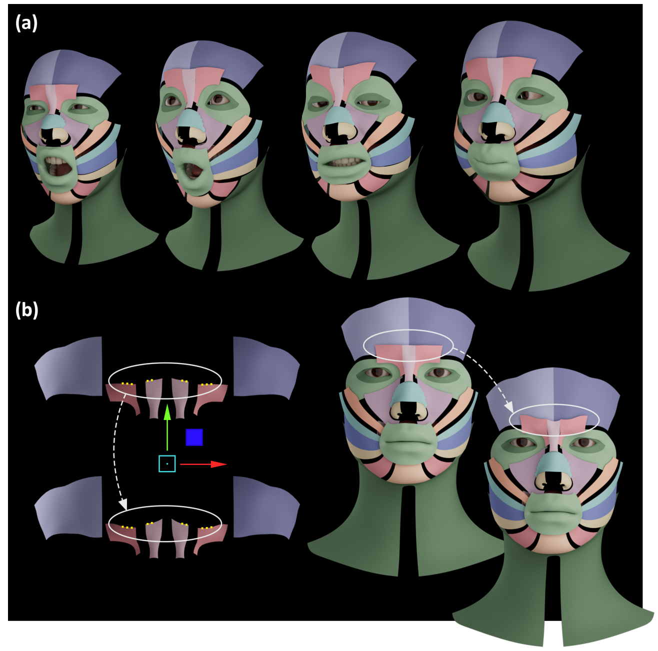

Fig. 4. A Fabrig parameterized face can be easily edited through: (a) manipulating the muscle blendshape weights; (b) adjusting the vertices on the muscle blendshapes to tune the muscle contraction intensity.

Editability and Performance Drivability. Our result shows that we can edit Fabrig-parameterized faces by manipulating the muscle blendshape weights (Figure 4.a). Artists can also edit the muscle blendshapes to tune their contraction intensities (Figure 4.b). Fabrig is fully compatible with facial motions annotated by FACS AUs. Figure 6 also demonstrates Fabrig parameterized faces being automatically animated by marker-based mocap data, where mocap data was translated into FACS AUs and their intensities to drive the muscle blendshapes and enable animation. The eyeballs were manually animated for demonstration.

5.3 Subjective Evaluation – A User Study

Subjective evaluation should also be considered for the feasibility of a face parameterization method. The most mentioned keywords in relevant research are facial actions' naturalness and semantic accuracy [Cao et al. 2013; Chaudhuri et al. 2019; Curio et al. 2006; Kim et al. 2021; Stoiber et al. 2010]. Therefore, we conduct user study to investigate if the facial actions presented by Fabrig parameterized faces are considered natural and reflect the mocap subjects' expressions accurately. This evaluation corresponds to the visual plausibility and semantic accuracy of our design objectives.

Within the user study, we applied the *Facial Action Set* to the *3D Scan Face Set* parameterized by MetaHuman Creator [EpicGames 2023] and by Fabrig. We showed these comparisons through a triplet display and asked users to rate the naturalness and semantic accuracy of the expressions from both versions on a scale of 1 to 5. Figure 5 is an example of the triplet we used in the user study. We ran the study with 20 adult participants and collected 20 valid responses.

Fig. 5. An example of the triplet used in our user study. The two 3D faces are parameterized by MetaHuman Creator (left) and Fabrig (right), and in the middle is the mocap video of the subject's performance.

We conducted a T-test [Kim 2015] to understand the difference in the scores of the two methods, our result (Table 4) shows that the score of the MetaHuman Creator parameterized 3D faces does not show a statistically significant difference from Fabrig parameterized faces in terms of the facial action's naturalness and semantic accuracy. This result confirms that Fabrig is comparable to a commercial blendshape-based parameterization method in visual plausibility and expressiveness when using the same face mesh under the same rendering setup. Yet unlike MetaHuman Creator, which is only capable of parameterizing realistic human characters, Fabrig can parameterize non-human characters.

Table 4. Mean scores and standard deviations of facial actions' naturalness and semantic accuracy on faces parameterized by MetaHuman Creator vs. Fabrig on a scale of 1 to 5.

Measures	MetaHuman	Fabrig	T-test p
Naturalness	3.982±**0.235**	**3.992**±0.298	0.424
Semantic Accuracy	3.835±0.345	**3.908±0.323**	0.305

6 Conclusion

In this work, we present an anatomy-inspired 3D face parameterization method - Fabrig, which is independent of face-specific blendshapes or 3D scans and allows light-weight simulation of a face's physcis-based properties. Fabrig is constructed on a set of patches representing facial anatomical components like skull, muscles, and fats, and uses the original mesh as the skin surface. We take the muscle patches as the main active components and create a set of template muscle blendshapes for defining their deformation spaces. These template muscle blendshapes are transferable to the faces of human, human-like, and non-human characters. The passive movements of fat pads and the muscles' secondary motion are innovatively realized through cloth simulation, which enables high-fidelity facial details and physically interactable facial animation. Fabrig has high editability so that each muscle can be independently adjusted and its influence on the final face mesh remains natural. It is also drivable by mocap data or animated 3D faces if they are rigged based on FACS action units.

Our objective evaluation has shown that Fabrig-parameterized 3D faces can recreate facial poses of many types of characters with high accuracy, while being more than 30 times faster than the conventional rigging process. In subjective evaluation, our user study results indicate that Fabrig recreated facial poses are considered comparable with those created by the commercial face rigging tool - MetaHuman Creator, in terms of naturalness and semantic accuracy. Our work is not free of limitations, since the goal of this research is to design a fast and high-quality 3D face parameterization with physics-based properties for a wide range of characters, Fabrig does not focus on the accurate modelling of facial anatomical components but rather uses them as a medium to enable cross-character transferability and we have not tested Fabrig on highly stylized or animal-like characters. The facial details like wrinkles are automatically generated through the cloth simulation, therefore might not be accurate to the wrinkle shapes of a live-action actor. High-frequency details, subject to a specific actor, are not yet realized with Fabrig. However, it is possible to assign a wrinkle map to a muscle cloth, which modifies the stretch and bend constraints of the cloth's influenced vertices and lets the cloth produce the desired skin details. In addition, more fat patches could be implemented with different cloth parameters to simulate effects such as Body Mass Index (BMI) change, aging and de-aging.

Acknowledgments

We sincerely thank Dr. Eric Paquette for his valuable feedback, our reviewers for their constructive comments, Mr. Andrew Roth and Mr. Paul Durocher for their technical support in our mocap and face scanning process. We also appreciate Ms. Francesca de Vries for her professional performance in many of our mocap sessions, Elis Joynes, Kylie Duck, and Ronan Boyd for their help during data collection. This work is supported by the NSERC CREATE Project VISION: VIsual effectS and animation InnovatiOn and simulatioN (584762).

References

Victoria Fernández Abrevaya, Adnane Boukhayma, Stefanie Wuhrer, and Edmond Boyer. 2019. A generative 3D facial model by adversarial training. In *Proc. International Conference on Computer Vision (ICCV)*.

Timur Bagautdinov, Chenglei Wu, Jason Saragih, Pascal Fua, and Yaser Sheikh. 2018. Modeling facial geometry using compositional vaes. In *Proceedings of the IEEE Conference on Computer Vision and Pattern Recognition*. 3877–3886.

Kevin Baker. 2019. How Much Does It Cost to Create A 3D Model of A Main Character Such As Frozen's Elsa? https://www.quora.com/How-much-does-it-cost-to-create-a-3D-model-of-a-main-character-such-as-Frozens-Elsa Accessed: September 11, 2024.

Linchao Bao, Xiangkai Lin, Yajing Chen, Haoxian Zhang, Sheng Wang, Xuefei Zhe, Di Kang, Haozhi Huang, Xinwei Jiang, Jue Wang, et al. 2021. High-fidelity 3d digital human head creation from rgb-d selfies. *ACM Transactions on Graphics (TOG)* 41, 1 (2021), 1–21.

Michael Bao, Matthew Cong, Stéphane Grabli, and Ronald Fedkiw. 2019. High-quality face capture using anatomical muscles. In *Proceedings of the IEEE/CVF Conference on Computer Vision and Pattern Recognition*. 10802–10811.

David Baraff and Andrew Witkin. 2023. Large steps in cloth simulation. In *Seminal Graphics Papers: Pushing the Boundaries, Volume 2*. 767–778.

Vincent Barrielle, Nicolas Stoiber, and Cédric Cagniart. 2016. Blendforces: A dynamic framework for facial animation. In *Computer Graphics Forum*, Vol. 35. Wiley Online Library, 341–352.

Volker Blanz, Curzio Basso, Tomaso Poggio, and Thomas Vetter. 2003. Reanimating faces in images and video. In *Computer graphics forum*, Vol. 22. Wiley Online Library, 641–650.

Volker Blanz and Thomas Vetter. 2023. A morphable model for the synthesis of 3D faces. In *Seminal Graphics Papers: Pushing the Boundaries, Volume 2*. 157–164.

Blender. 2023. Blender. https://www.blender.org/ Accessed: September 11, 2024.

Chen Cao, Yanlin Weng, Shun Zhou, Yiying Tong, and Kun Zhou. 2013. Facewarehouse: A 3d facial expression database for visual computing. *IEEE Transactions on*

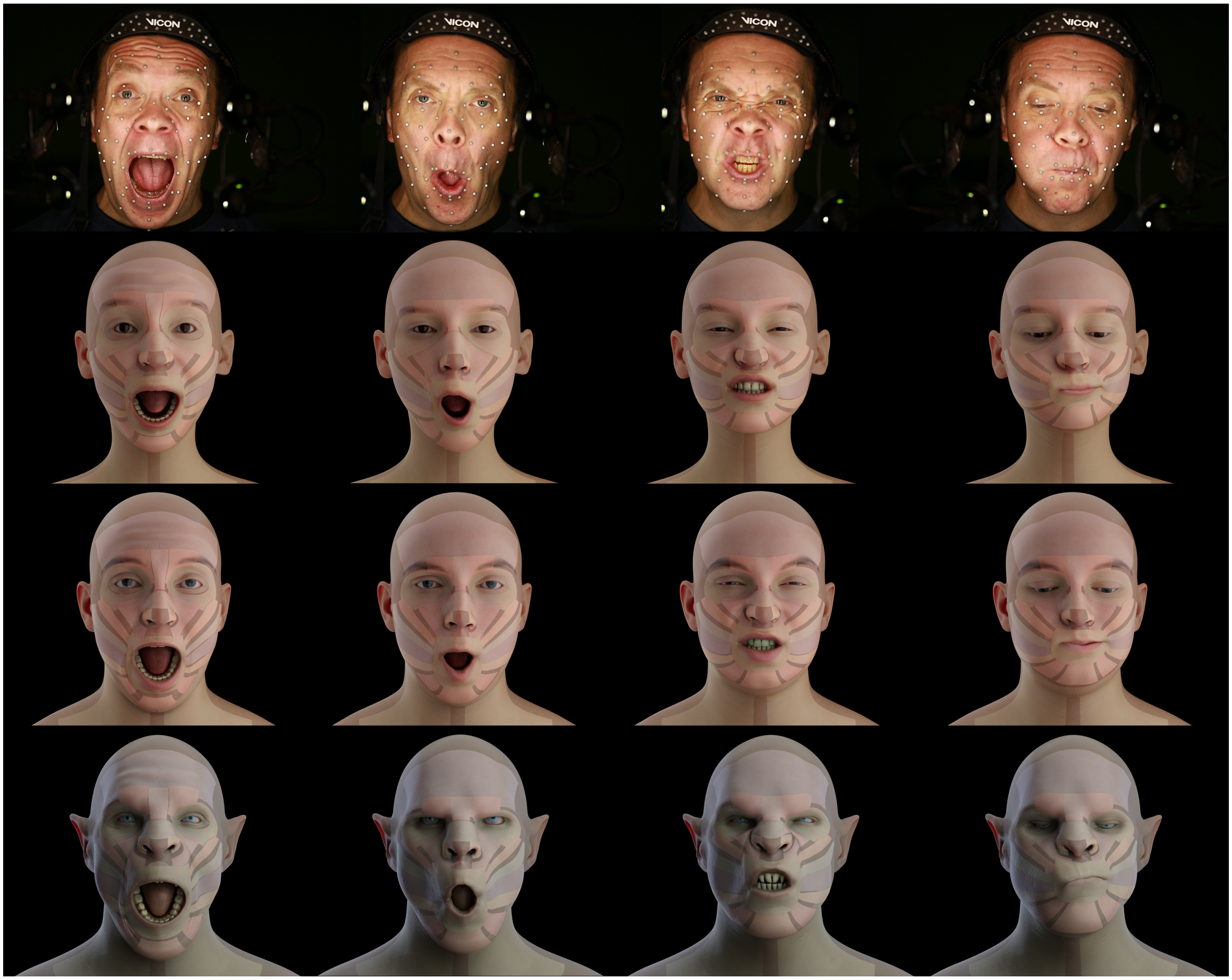

Fig. 6. An example of Fabrig parameterized faces being animated by marker-based mocap data. (Orc model credit [TheWho 2017])

Visualization and Computer Graphics 20, 3 (2013), 413–425.

Prashanth Chandran, Loïc Ciccone, Markus Gross, and Derek Bradley. 2022. Local anatomically-constrained facial performance retargeting. *ACM Transactions on Graphics (TOG)* 41, 4 (2022), 1–14.

Prashanth Chandran and Gaspard Zoss. 2024. Anatomically Constrained Implicit Face Models. In *Proceedings of the IEEE/CVF Conference on Computer Vision and Pattern Recognition*. 2220–2229.

Bindita Chaudhuri, Noranart Vesdapunt, Linda Shapiro, and Baoyuan Wang. 2020. Personalized face modeling for improved face reconstruction and motion retargeting. In *Computer Vision–ECCV 2020: 16th European Conference, Glasgow, UK, August 23–28, 2020, Proceedings, Part V 16*. Springer, 142–160.

Bindita Chaudhuri, Noranart Vesdapunt, and Baoyuan Wang. 2019. Joint face detection and facial motion retargeting for multiple faces. In *Proceedings of the IEEE/CVF Conference on Computer Vision and Pattern Recognition*. 9719–9728.

Byoungwon Choe, Hanook Lee, and Hyeong-Seok Ko. 2001. Performance-driven muscle-based facial animation. *The Journal of Visualization and Computer Animation* 12, 2 (2001), 67–79.

Byungkuk Choi, Haekwang Eom, Benjamin Mouscadet, Stephen Cullingford, Kurt Ma, Stefanie Gassel, Suzi Kim, Andrew Moffat, Millicent Maier, Marco Revelant, et al. 2022. Animatomy: An animator-centric, anatomically inspired system for 3d facial modeling, animation and transfer. In *SIGGRAPH Asia 2022 Conference Papers*. 1–9.

Matthew Cong, Michael Bao, Jane L E, Kiran S Bhat, and Ronald Fedkiw. 2015. Fully automatic generation of anatomical face simulation models. In *Proceedings of the 14th ACM SIGGRAPH/Eurographics Symposium on Computer Animation*. 175–183.

Matthew Cong and Ronald Fedkiw. 2019. Muscle-based facial retargeting with anatomical constraints. In *ACM SIGGRAPH 2019 Talks*. 1–2.

Matthew Deying Cong. 2016. *Art-directed muscle simulation for high-end facial animation*. Ph. D. Dissertation. Stanford University.

Cristóbal Curio, Martin Breidt, Mario Kleiner, Quoc C Vuong, Martin A Giese, and Heinrich H Bülthoff. 2006. Semantic 3d motion retargeting for facial animation. In *Proceedings of the 3rd Symposium on Applied Perception in Graphics and Visualization*. 77–84.

Bernhard Egger, William AP Smith, Ayush Tewari, Stefanie Wuhrer, Michael Zollhoefer, Thabo Beeler, Florian Bernard, Timo Bolkart, Adam Kortylewski, Sami Romdhani, et al. 2020. 3d morphable face models—past, present, and future. *ACM Transactions on Graphics (ToG)* 39, 5 (2020), 1–38.

Paul Ekman and Wallace V Friesen. 1978. *Facial action coding systems*. Consulting Psychologists Press.

EpicGames. 2023. MetaHuman: Hign-fidelity Digital Humans Made Easy. https://www.unrealengine.com/en-US/metahuman Accessed: September 11, 2024.

Aurel Gruber, Marco Fratarcangeli, Gaspard Zoss, Roman Cattaneo, Thabo Beeler, Markus Gross, and Derek Bradley. 2020. Interactive sculpting of digital faces using

an anatomical modeling paradigm. *Computer Graphics Forum* 39, 5 (2020), 93–102.
Alexandru-Eugen Ichim, Petr Kadleček, Ladislav Kavan, and Mark Pauly. 2017. Phace: Physics-based face modeling and animation. *ACM Transactions on Graphics (TOG)* 36, 4 (2017), 1–14.
Alexandru Eugen Ichim, Ladislav Kavan, Merlin Nimier-David, and Mark Pauly. 2016. Building and animating user-specific volumetric face rigs. In *Symposium on Computer Animation*. 107–117.
Seonghyeon Kim, Sunjin Jung, Kwanggyoon Seo, Roger Blanco i Ribera, and Junyong Noh. 2021. Deep learning-based unsupervised human facial retargeting. In *Computer Graphics Forum*, Vol. 40. Wiley Online Library, 45–55.
Tae Kyun Kim. 2015. T test as a parametric statistic. *Korean journal of anesthesiology* 68, 6 (2015), 540.
John P Lewis, Ken Anjyo, Taehyun Rhee, Mengjie Zhang, Frederic H Pighin, and Zhigang Deng. 2014. Practice and theory of blendshape facial models. *Eurographics (State of the Art Reports)* 1, 8 (2014), 2.
Ruilong Li, Karl Bladin, Yajie Zhao, Chinmay Chinara, Owen Ingraham, Pengda Xiang, Xinglei Ren, Pratusha Prasad, Bipin Kishore, Jun Xing, et al. 2020. Learning formation of physically-based face attributes. In *Proceedings of the IEEE/CVF conference on computer vision and pattern recognition*. 3410–3419.
Tianye Li, Timo Bolkart, Michael J Black, Hao Li, and Javier Romero. 2017. Learning a model of facial shape and expression from 4D scans. *ACM Trans. Graph.* 36, 6 (2017), 194–1.
Samuel Marcos, Jaime G Garcia Bermejo, and Eduardo Zalama. 2008. A realistic facial animation suitable for human-robot interfacing. In *2008 IEEE/RSJ International Conference on Intelligent Robots and Systems*. IEEE, 3810–3815.
David Matsumoto and Paul Ekman. 2008. Facial expression analysis. *Scholarpedia* 3, 5 (2008), 4237.
Tim Milliron, Robert J Jensen, Ronen Barzel, and Adam Finkelstein. 2002. A framework for geometric warps and deformations. *ACM Transactions on Graphics (TOG)* 21, 1 (2002), 20–51.
Masahiro Mori. 1970. The uncanny valley: the original essay by Masahiro Mori. *IEEE Spectrum* 6 (1970).
Lucio Moser, Chinyu Chien, Mark Williams, Jose Serra, Darren Hendler, and Doug Roble. 2021. Semi-supervised video-driven facial animation transfer for production. *ACM Transactions on Graphics (TOG)* 40, 6 (2021), 1–18.
Matthias Müller, Bruno Heidelberger, Marcus Hennix, and John Ratcliff. 2007. Position based dynamics. *Journal of Visual Communication and Image Representation* 18, 2 (2007), 109–118.
Verónica Orvalho, Pedro Bastos, Frederic I Parke, Bruno Oliveira, and Xenxo Alvarez. 2012. A Facial Rigging Survey. *Eurographics (State of the Art Reports)* (2012), 183–204.
Verónica Costa Orvalho, Ernesto Zacur, and Antonio Susin. 2008. Transferring the rig and animations from a character to different face models. In *Computer Graphics Forum*, Vol. 27. Wiley Online Library, 1997–2012.
Wolfgang Paier, Anna Hilsmann, and Peter Eisert. 2023. Unsupervised Learning of Style-aware Facial Animation from Real Acting Performances. *Graphical Models* 129 (2023), 101199.
Dafei Qin, Jun Saito, Noam Aigerman, Thibault Groueix, and Taku Komura. 2023. Neural Face Rigging for Animating and Retargeting Facial Meshes in the Wild. *arXiv preprint arXiv:2305.08296* (2023).
Zesong Qiu, Yuwei Li, Dongming He, Qixuan Zhang, Longwen Zhang, Yinghao Zhang, Jingya Wang, Lan Xu, Xudong Wang, Yuyao Zhang, et al. 2022. SCULPTOR: Skeleton-consistent face creation using a learned parametric generator. *ACM Transactions on Graphics (TOG)* 41, 6 (2022), 1–17.
Roger Blanco I Ribera, Eduard Zell, John P Lewis, Junyong Noh, and Mario Botsch. 2017. Facial retargeting with automatic range of motion alignment. *ACM Transactions on graphics (TOG)* 36, 4 (2017), 1–12.
Yeongho Seol, John P Lewis, Jaewoo Seo, Byungkuk Choi, Ken Anjyo, and Junyong Noh. 2012. Spacetime expression cloning for blendshapes. *ACM Transactions on Graphics (TOG)* 31, 2 (2012), 1–12.
Yeongho Seol, Jaewoo Seo, Paul Hyunjin Kim, John P Lewis, and Junyong Noh. 2011. Artist friendly facial animation retargeting. *ACM Transactions on Graphics (TOG)* 30, 6 (2011), 1–10.
Mincheol Shin, Se Jung Kim, and Frank Biocca. 2019. The uncanny valley: No need for any further judgments when an avatar looks eerie. *Computers in Human Behavior* 94 (2019), 100–109.
Eftychios Sifakis, Igor Neverov, and Ronald Fedkiw. 2005. Automatic determination of facial muscle activations from sparse motion capture marker data. In *ACM SIGGRAPH 2005 Papers*. 417–425.
Sangeetha Grama Srinivasan, Qisi Wang, Junior Rojas, Gergely Klár, Ladislav Kavan, and Eftychios Sifakis. 2021. Learning active quasistatic physics-based models from data. *ACM Transactions on Graphics (TOG)* 40, 4 (2021), 1–14.
Jos Stam. 2009. Nucleus: Towards a unified dynamics solver for computer graphics. In *2009 11th IEEE International Conference on Computer-Aided Design and Computer Graphics*. IEEE, 1–11.
Nicolas Stoiber, Renaud Seguier, and Gaspard Breton. 2010. Facial animation retargeting and control based on a human appearance space. *Computer animation and virtual worlds* 21, 1 (2010), 39–54.
Demetri Terzopoulos and Keith Waters. 1990. Physically-based facial modelling, analysis, and animation. *The journal of visualization and computer animation* 1, 2 (1990), 73–80.
TheWho. 2017. Azog Bust Likeness Study. https://skfb.ly/6sSzx. Accessed: September 11, 2024.
Justus Thies, Michael Zollhöfer, Matthias Nießner, Levi Valgaerts, Marc Stamminger, and Christian Theobalt. 2015. Real-time expression transfer for facial reenactment. *ACM Trans. Graph.* 34, 6 (2015), 183–1.
Luan Tran and Xiaoming Liu. 2018. Nonlinear 3d face morphable model. In *Proceedings of the IEEE conference on computer vision and pattern recognition*. 7346–7355.
Tamás Umenhoffer and Balázs Tóth. 2012. Facial animation retargeting framework using radial basis functions. In *Sixth Hungarian Conference on Computer Graphics and Geometry*. 64–69.
Nicolas Wagner, Mario Botsch, and Ulrich Schwanecke. 2023. SoftDECA: Computationally Efficient Physics-Based Facial Animations. In *Proceedings of the 16th ACM SIGGRAPH Conference on Motion, Interaction and Games*. 1–11.
Keith Waters. 1987. A muscle model for animation three-dimensional facial expression. *Acm siggraph computer graphics* 21, 4 (1987), 17–24.
Chenglei Wu, Derek Bradley, Markus Gross, and Thabo Beeler. 2016. An anatomically-constrained local deformation model for monocular face capture. *ACM transactions on graphics (TOG)* 35, 4 (2016), 1–12.
Menghua Wu, Hao Zhu, Linjia Huang, Yiyu Zhuang, Yuanxun Lu, and Xun Cao. 2023. High-Fidelity 3D Face Generation From Natural Language Descriptions. In *Proceedings of the IEEE/CVF Conference on Computer Vision and Pattern Recognition*. 4521–4530.
Haotian Yang, Hao Zhu, Yanru Wang, Mingkai Huang, Qiu Shen, Ruigang Yang, and Xun Cao. 2020. Facescape: a large-scale high quality 3d face dataset and detailed riggable 3d face prediction. In *Proceedings of the ieee/cvf conference on computer vision and pattern recognition*. 601–610.
Lingchen Yang, Byungsoo Kim, Gaspard Zoss, Baran Gözcü, Markus Gross, and Barbara Solenthaler. 2022. Implicit Neural Representation for Physics-driven Actuated Soft Bodies. *ACM Transactions on Graphics (TOG)* 41, 4 (2022), 1–10.
Lingchen Yang, Gaspard Zoss, Prashanth Chandran, Paulo Gotardo, Markus Gross, Barbara Solenthaler, Eftychios Sifakis, and Derek Bradley. 2023. An Implicit Physical Face Model Driven by Expression and Style. In *SIGGRAPH Asia 2023 Conference Papers*. 1–12.
Juyong Zhang, Keyu Chen, and Jianmin Zheng. 2020. Facial expression retargeting from human to avatar made easy. *IEEE Transactions on Visualization and Computer Graphics* 28, 2 (2020), 1274–1287.
Longwen Zhang, Chuxiao Zeng, Qixuan Zhang, Hongyang Lin, Ruixiang Cao, Wei Yang, Lan Xu, and Jingyi Yu. 2022. Video-driven Neural Physically-based Facial Asset for Production. *ACM Transactions on Graphics (TOG)* 41, 6 (2022), 1–16.
Longwen Zhang, Zijun Zhao, Xinzhou Cong, Qixuan Zhang, Shuqi Gu, Yuchong Gao, Rui Zheng, Wei Yang, Lan Xu, and Jingyi Yu. 2023. Hack: Learning a parametric head and neck model for high-fidelity animation. *ACM Transactions on Graphics (TOG)* 42, 4 (2023), 1–20.
ChangAn Zhu and Chris Joslin. 2024. A review of motion retargeting techniques for 3D character facial animation. *Computers & Graphics* (2024), 104037. https://doi.org/10.1016/j.cag.2024.104037
Olgierd Cecil Zienkiewicz and Robert Leroy Taylor. 2000. *The finite element method: solid mechanics*. Vol. 2. Butterworth-heinemann.
Gaspard Zoss, Derek Bradley, Pascal Bérard, and Thabo Beeler. 2018. An empirical rig for jaw animation. *ACM Transactions on Graphics (TOG)* 37, 4 (2018), 1–12.